Multiplicity of steady states in cylindrical Rayleigh-Bénard convection

Dong-Jun Ma, De-Jun Sun, and Xie-Yuan Yin
School of Engineering Science, University of Science and Technology of China, Hefei 230027, China
(Received 13 June 2006; published 22 September 2006)

Three-dimensional steady Rayleigh-Bénard convection in a vertical cylinder is investigated by numerical simulation and bifurcation analysis. The complex pattern formation beyond the onset of the convection is presented by a bifurcation diagram. The coexistence of multiple stable states is observed near the threshold of the first bifurcation and two group symmetries are summarized for the corresponding primary branches. The first stable target pattern originates through a subcritical bifurcation. A multiplicity of flow states for the Rayleigh number of 14 200 is validated numerically in comparison with the experiment, and a four-spoke pattern is observed.

DOI: 10.1103/PhysRevE.74.037302 PACS number(s): 47.20.Ky, 47.20.Bp, 47.54.−r

Rayleigh-Bénard convection in a fluid layer heated from below and cooled from above provides rich instances of complex pattern formation and constitutes a high-dimensional nonlinear system for transition to chaos and turbulence. It has been a subject of numerous experimental and theoretical investigations [1–4] for classifying and characterizing the various convection patterns according to their spatial and temporal behavior. The important applications are in, e.g., meteorology, geophysics, astrophysics, crystal growth, and industrial processes.

The occurrence of various convective patterns in a circular cylindrical cavity, partly coexisting simultaneously for the same values of control parameters, was observed in many experiments [4–9] and investigated by theoretical analyses [2,10,11] and numerical simulations [12–18]. The primary instabilities of the trivial conductive solution have been well studied by linear analysis [12,14,15]. The critical Rayleigh number is a function of the aspect ratio, and approaches the limit value of 1708 with increasing aspect ratio. The fluid motion that evolves for Rayleigh numbers beyond the critical values is highly nonlinear and depends strongly on the aspect ratio and the Prandtl number, where even weak nonlinear solutions cannot predict the secondary bifurcation correctly [14–16]. Hof *et al.* [9] considered a small aspect ratio experiment which demonstrates that both axisymmetric and asymmetric steady flows can exist for the same aspect ratio of order unity. However, the various flow patterns in this experiment are not completely verified by a numerical study [18] with the same configuration. Because of the multiplicity of steady states in this situation, it is difficult to predict the pattern formation and determine all the stable solutions by either experiment or direct numerical simulation.

Bifurcation theory [11] has long been a very helpful tool in the analysis of the complex dynamics of nonlinear systems, such as the case of Rayleigh-Bénard convection. If symmetries are present, group methods are also an important assistance to the theoretical analysis. In order to capture all the stable and unstable states of the system, the numerical bifurcation method is facilitated with eigenvalue calculations at given equilibrium states for stability analysis and path following of solution branches to obtain the evolution of flow patterns.

In this Brief Report we use numerical simulation and bifurcation analysis to study the multiplicity of steady states for an aspect ratio (radius to height) of 2 and a Prandtl number of 6.7, in corresponding with the experiment in Ref. [9]. Particular attention is paid to the symmetry and symmetry breaking of the system.

We consider the thermal convection in a vertical cylindrical cavity of aspect ratio $a=R/H$, where H is the height and R is the radius of the cavity. A temperature difference $\Delta T=T_h-T_c$ is maintained between the bottom and top boundaries. The dimensionless equations in Boussinesq approximation explicitly read

$$\nabla \cdot \mathbf{u} = 0, \tag{1}$$

$$\partial_t \mathbf{u} + \mathbf{u} \cdot \nabla \mathbf{u} = -\nabla p + \nabla^2 \mathbf{u} + (\mathrm{Ra}/\mathrm{Pr})\theta \hat{\boldsymbol{z}}, \tag{2}$$

$$\partial_t \theta + \mathbf{u} \cdot \nabla \theta = (1/\mathrm{Pr})\nabla^2 \theta, \tag{3}$$

where $\mathbf{u}=(u_r,u_\varphi,u_z)$ is the velocity field in (r,φ,z) cylindrical coordinates. θ denotes the dimensionless temperature $(T-T_c)/(T_h-T_c)$. The length, time, and velocity are scaled by H, H^2/ν, and ν/H, respectively, where ν is the kinematic viscosity. The dimensionless parameters are the Prandtl number $\mathrm{Pr}=\nu/\kappa$, and the Rayleigh number $\mathrm{Ra}=g\beta\Delta T H^3/(\kappa\nu)$, where κ denotes the thermal diffusivity, g the gravity level, β the thermal expansion coefficient. In correspondence with the experiments without external sidewall forcing, the nonslip boundary condition is prescribed at all the container walls, the temperature is fixed at the top and bottom planes, and the normal heat flux is zero along the lateral wall.

Due to the cylindrical geometry, the Boussinesq equations (1)–(3) are invariant with respect to the $\mathcal{O}(2)\times\mathcal{Z}_2$ symmetry [19], where the $\mathcal{O}(2)$ group contains the rotation symmetry around the z axis and the reflection symmetry with respect to the vertical planes containing this axis, and the $\mathcal{Z}_2$ group corresponds to the reflection symmetry with respect to the horizontal midplane. Symmetries have important consequences on the nature of possible bifurcations, because the image of a solution through a broken symmetry is also a solution to the system.

The time-dependent solutions of Eqs. (1)–(3) are obtained by using a second-order fractional-step method in three-dimensional cylindrical coordinates, which is an improved version of the algorithm in Refs. [20,21] with an additional

TABLE I. Comparison of the thresholds of the second bifurcation for $a=1$ with mesh $32\times48\times32$.

Pr	Ref. [15]	Ref. [16]	Present
1 ($m=2$)	3017	2969	2992
6.7 ($m=1$)	10134	12370	11950

pressure predictor step as in Ref. [22]. Based on this algorithm, a first-order time-stepping formulation can be utilized to calculate both stable and unstable steady solutions and analyze their stability, as described in Refs. [16,23–25]. In order to validate our codes, we calculate some typical thresholds of the bifurcations for aspect ratio $a=1$. The convection sets in with the axisymmetric mode at $\mathrm{Ra}_{cr}=2256$, which agrees well with the linear stability result ($\mathrm{Ra}_{cr}=2260$ [13,14]). In Table I, we compare our values of the secondary thresholds with those results in the previous literature. Agreement on the axisymmetry-breaking bifurcation is also obtained. In the present research, the values of the parameters are Pr=6.7 and $a=2$, close to those characteristic of the experiment [9]. The spatial discretization uses typically $40\times64\times20$ mesh grid points in the (r,φ,z) directions, which is near that in Ref. [18].

The scenario provided by the analysis of the steady solutions is shown in the bifurcation diagram of Fig. 1. In this figure the Nusselt number Nu, representing heat transfer from the heated lower wall to the cooled upper wall, is evaluated as a function of the Rayleigh number. In correspondence with this diagram, we present in Fig. 2 all the stable and unstable flow patterns of the branches bifurcating from the trivial conductive solution, and in Table II the critical Rayleigh numbers for the onset of various flow patterns. The corresponding patterns can be characterized by the Fourier modes and their broken symmetries with regard to the symmetries of the problem. The resulting subsymmetry can

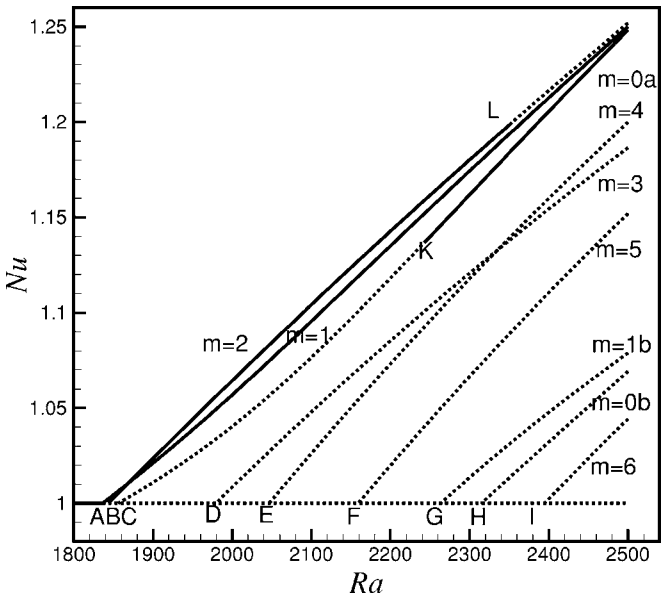

FIG. 1. Bifurcation diagram for the Nusselt number vs Ra. Continuous lines: Stable states. Dashed lines: Unstable states.

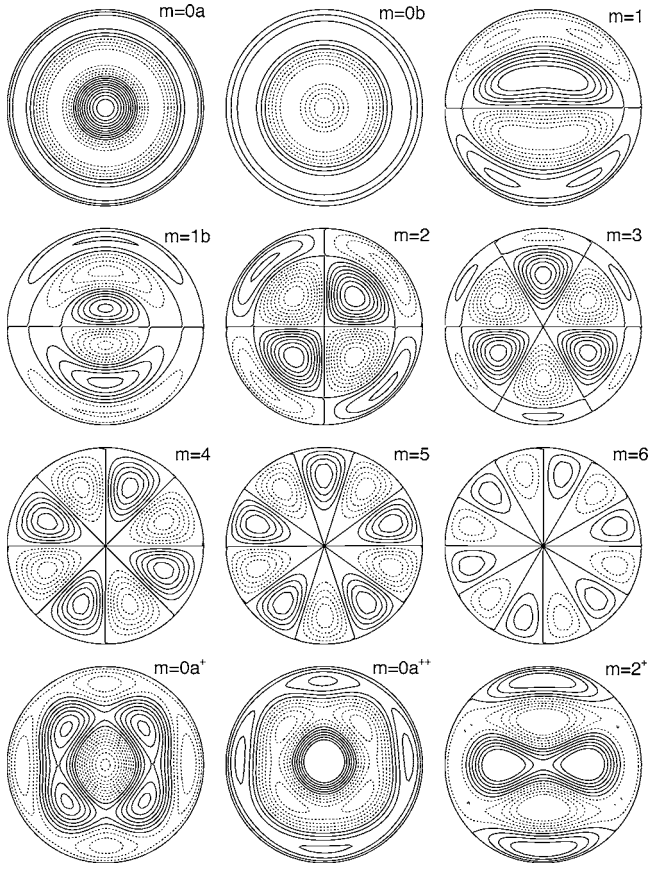

FIG. 2. Flow patterns at Ra=2500: Contours of the vertical velocity in the horizontal midplane (dashed lines correspond to negative values).

be generalized by four groups of discrete transformations: the horizontal midplane reflection γ, the reflection κ with respect to the vertical plane in which no azimuthal motion exists, the rotation by π/m about this plane denoted by $R_{\pi/m}$, and the dihedral group D_m consisting of the repetitions of a proper rotation by $2\pi/m$ and the reflections in m planes forming angles of π/m. For the sake of clarity only one solution of each branch has been shown, because both the patterns and their inverse equivalents can be deduced from the broken reflection symmetry with respect to the horizontal midplane P_H, and the pitchfork bifurcation generates an infinite number of equivalent solutions parametrized by phase when the $\mathcal{O}(2)$ symmetry is broken with azimuthal wave number $m\neq0$.

First, we consider the primary bifurcations from the conductive solution. For small Rayleigh numbers the system without motion is stable, but loses stability to three-

TABLE II. Critical Rayleigh numbers for the onset of flow patterns.

Mode	Ra_{cr}	Mode	Ra_{cr}	Mode	Ra_{cr}	Mode	Ra_{cr}
1	1836	3	1979	1*b*	2263	2^+	2350
2	1844	4	2045	0*b*	2314	$0a^+$	2113
0*a*	1856	5	2159	6	2395	$0a^{++}$	2245

dimensional convection with an asymmetric mode ($m=1$) through a supercritical pitchfork bifurcation at Ra=1836 (A in Fig. 1), which agrees well with the result of $\mathrm{Ra}_{cr}=1832$ by linear stability analysis [14]. As shown in Fig. 2 by the contours of vertical velocity in the plane P_H, this flow pattern consists of one main roll at the center of the cylinder with two weaker half-circular rolls, where the symmetries preserved are $\kappa, \gamma R_\pi, \kappa\gamma R_\pi$. Near the onset of convection, the second mode ($m=2$) of the primary bifurcation appears soon at Ra=1844 (B in Fig. 1), which is also stable with symmetries of $D_2, \gamma R_{\pi/2}, \gamma R_{\pi/2} D_2$. The structure of the inner four rolls is similar to the same mode for $a=1$ in Ref. [16]: the fluid ascends in two opposite quadrants and descends in the two others. Meanwhile, an additional four rolls form near the sidewall due to the increasing aspect ratio. The third mode ($m=0a$) is an axisymmetric mode with $\mathcal{O}(2)$ symmetry, but it is unstable. This target pattern has two concentric circular rolls, where the fluid descends in the middle of the radius and rises near the axis and along the wall, respectively, as shown in Fig. 2. All the following six modes of the primary bifurcation are unstable including four high wave number modes (from 3 to 6), the axisymmetric mode ($m=0b$) with a single circular roll, and another asymmetric mode ($m=1b$) with five rolls. The patterns with high wave number $m=4,5,6$ have similar flow structures including $2m$ rolls, which are different from the low wave number cases with additional weak rolls near the wall. If D_1 denotes the bilateral symmetry κ, the symmetries of the primary branches bifurcating from the conductive solution can be reduced to two groups: $\mathcal{O}(2)$ symmetry for axisymmetric modes, and symmetries of $D_m, \gamma R_{\pi/m}, \gamma R_{\pi/m} D_m$ for asymmetric modes.

Complex secondary bifurcations originate even near the onset of convection. Above the threshold value of Ra =2113 (J in Fig. 3), the axisymmetric solution bifurcates to a new asymmetric mode denoted by $m=0a^+$, which is still unstable, and the $\mathcal{O}(2)$ symmetry is broken to the subsymmetries of κ and R_π with two symmetric planes. This is D_2 symmetry. The following bifurcation of the axisymmetric branch is subcritical, the axisymmetric solution with two concentric circular rolls becomes stable while another unstable asymmetric branch appears at Ra=2245 (K). The new unstable mode $m=0a^{++}$ loses almost all the symmetries besides the κ symmetry with only one symmetric plane. The flow structure of $m=0a^{++}$ is almost the same as that of $m=0a^+$, but with a biased center which destroys one κ symmetry. Above the threshold of the subcritical bifurcation, stable axisymmetric and asymmetric solutions exist at the same time, which is not far from the onset of convection. Just after the subcritical bifurcation, a new supercritical bifurcation is observed at Ra=2350 (L) for the branch of $m=2$. The eight-roll solution loses its stability and bifurcates to a new stable solution with six main rolls, which breaks the γ symmetry with respect to the horizontal midplane P_H and preserves the D_2 symmetry.

When the Rayleigh number exceeds 2500, it is very difficult to follow all the branches because the new stable or unstable solutions will emerge continuously from the high-level bifurcations, and also from the primary bifurcation with higher wave numbers. Only following the stable branches and their corresponding bifurcations may be a realistic way for future research.

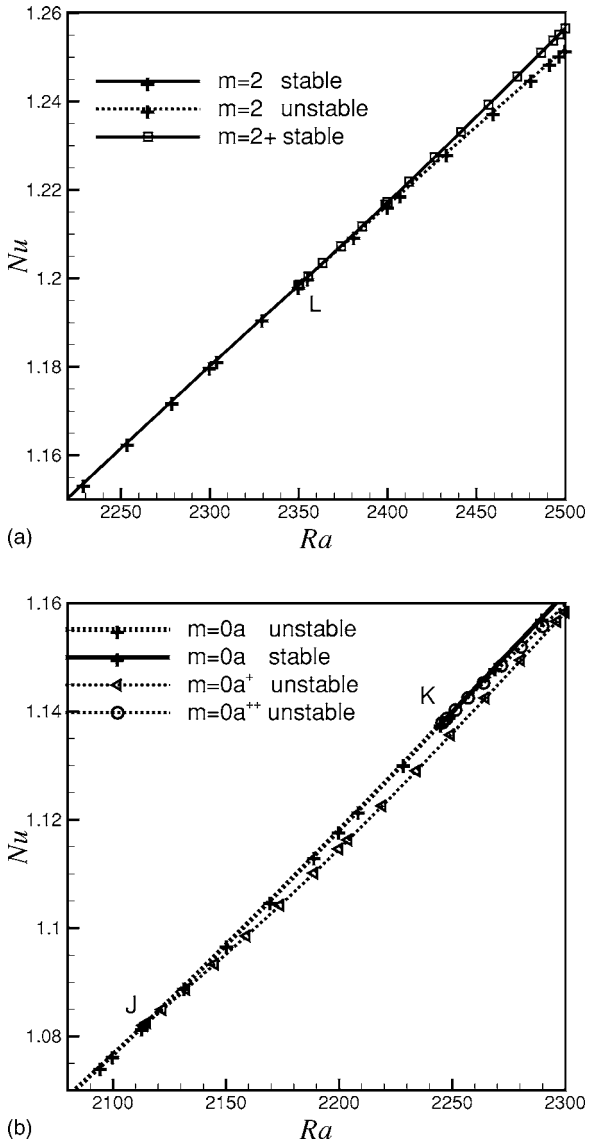

FIG. 3. Supercritical (a) and subcritical (b) bifurcations. Continuous lines: Stable states. Dashed lines: Unstable states.

In comparison with the experiment of flow state multiplicity in Ref. [9], the steady solutions at Ra=14 200 are calculated with different initial conditions. The steady target, parallel rolls, and spoke flow patterns are shown in Fig. 4. The axisymmetric pattern with one circular roll is shown in Fig. 4(a), where the fluid descends in the center and ascends along the sidewall. The pattern of the inverse equivalent in Ref. [9] is not given here. Note that this solution with $\mathcal{O}(2)$ symmetry is on the axisymmetric branch of $m=0b$ which is unstable for small Rayleigh number, whereas the above flow pattern of axisymmetric mode $m=0a$ disappears here due to a fold bifurcation. Figure 4(b) gives the two-roll pattern with cold fluid falling along the center. Figures 4(c) and 4(d) show the three-roll and four-roll patterns, which have better symmetry than the shadowgraph images in the experiment [9]. The flow patterns in Figs. 4(b) and 4(d) are of D_2 symmetry; nevertheless Fig. 4(c) preserves $\kappa, \gamma R_\pi, \kappa\gamma R_\pi$ symmetry. The

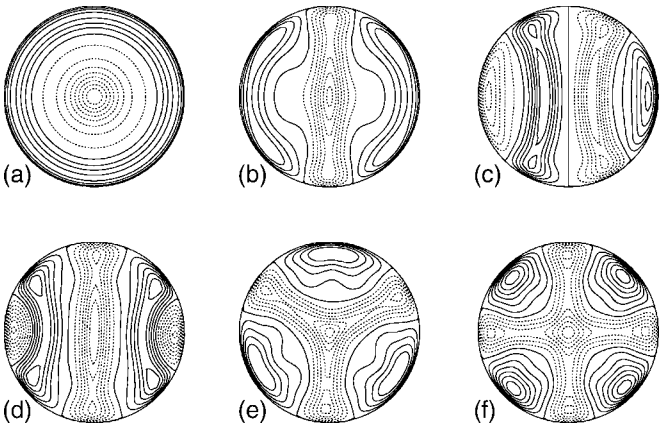

FIG. 4. Multiplicity of flow states at Ra=14 200 in comparison with the experiment [9].

three-spoke pattern with cold fluid descending along the spokes is D_3 symmetric as shown in Fig. 4(e). In addition to these patterns, which have been observed in experiment [9], a pair of four-spoke patterns with D_4 symmetry is found by numerical analysis. As shown in Fig. 4(f), the flow pattern consists of four central spokes corresponding with the downward motion while four upward-flowing jets exist near the sidewall between the spokes. The reversed pattern can also be observed with the same parameters.

In conclusion, three-dimensional steady Rayleigh-Bénard convection with $a=2$ and Pr=6.7 has been investigated by numerical bifurcation techniques; the parameters correspond to the experiment of flow state multiplicity in Ref. [9]. Twelve types of convective patterns have been observed near the onset of convection when the Rayleigh number is less than 2500. The complex pattern formation is presented through bifurcation diagrams. The emerging flow corresponds to an asymmetric solution ($m=1$) at Ra=1836 by a supercritical pitchfork bifurcation. A multiplicity of steady states appears soon due to a second stable branch ($m=2$) of the primary bifurcation at Ra=1844. The symmetries of the primary branches bifurcated from the static solution can be reduced to two groups: $\mathcal{O}(2)$ symmetry for axisymmetric modes and symmetries of D_m, $\gamma R_{\pi/m}$, $\gamma R_{\pi/m} D_m$ for asymmetric modes. Above the threshold (Ra=2245) of subcritical bifurcation for the onset of stable target pattern, stable axisymmetric and asymmetric solutions coexist close to the onset of convection. Furthermore, multiple solutions for the Rayleigh number of 14 200 are validated numerically, and a four-spoke pattern is observed that has not been found in experiment.

[1] F. H. Busse, in *Hydrodynamic Instability and the Transition to Turbulence*, edited by H. L. Swinney and J. P. Gollub, Topics in Applied Physics Vol. 45 (Springer-Verlag, Berlin, 1984), p. 97.
[2] M. C. Cross and P. C. Hohenberg, Rev. Mod. Phys. **65**, 851 (1993).
[3] *Rayleigh-Bénard Convection, Structures and Dynamics*, edited by V. Getling, Advanced Series in Nonlinear Dynamics Vol. 11 (World Scientific, Singapore, 1995).
[4] E. Bodenschatz, W. Pesch, and G. Ahlers, Annu. Rev. Fluid Mech. **32**, 709 (2000).
[5] G. Müller, G. Neumann, and W. Weber, J. Cryst. Growth **70**, 78 (1984).
[6] G. Ahlers, D. S. Cannell, and V. Steinberg, Phys. Rev. Lett. **54**, 1373 (1985).
[7] M. Assenheimer and V. Steinberg, Nature (London) **367**, 345 (1994).
[8] R. V. Cakmur, D. A. Egolf, B. B. Plapp, and E. Bodenschatz, Phys. Rev. Lett. **79**, 1853 (1997).
[9] B. Hof, P. G. L. Lucas, and T. Mullin, Phys. Fluids **11**, 2815 (1999).
[10] J. C. Buell and I. Catton, Phys. Fluids **29**, 23 (1986).
[11] J. D. Crawford and E. Knobloch, Annu. Rev. Fluid Mech. **23**, 341 (1991).
[12] J. C. Buell and I. Catton, J. Heat Transfer **105**, 255 (1983).
[13] G. Neumann, J. Fluid Mech. **214**, 559 (1990).
[14] G. R. Hardin and R. L. Sani, Int. J. Numer. Methods Fluids **17**, 755 (1993).
[15] M. Wanschura, H. C. Kuhlmann, and H. J. Rath, J. Fluid Mech. **326**, 399 (1996).
[16] R. Touihri, H. Ben Hadid, and D. Henry, Phys. Fluids **11**, 2078 (1999).
[17] S. Rüdiger and F. Feudel, Phys. Rev. E **62**, 4927 (2000).
[18] S. S. Leong, Numer. Heat Transfer, Part A **41**, 673 (2002).
[19] *Singularities and Groups in Bifurcation Theory*, edited by M. Golubitsky, I. Stewart, and D. G. Schaeffer (Springer, New York, 1988), Vol. II.
[20] R. Verzicco and P. Orlandi, J. Comput. Phys. **123**, 402 (1996).
[21] D. J. Ma, D. Henry, and H. Ben Hadid, Phys. Fluids **17**, 124101 (2005).
[22] S. Hugues and A. Randriamampianina, Int. J. Numer. Methods Fluids **28**, 501 (1998).
[23] L. S. Tuckerman and D. Barkley, in *Numerical Methods for Bifurcation Problems and Large-Scale Dynamical Systems*, edited by E. Doedel and L. S. Tuckerman (Springer, New York, 2000), Vol. 119, pp. 453–466.
[24] E. Meca, I. Mercader, O. Batiste, and L. Ramirez-Piscina, Phys. Rev. Lett. **92**, 234501 (2004).
[25] D. J. Ma, D. J. Sun, and X. Y. Yin, Chin. Phys. Lett. **22**, 1964 (2005).